Evaluation of the Effect of Operating Parameters on the Performance of Orifice/Porous Pipe Type Micro-bubble Generator

Benny Arif Pambudiarto[1], Aswati Mindaryani[1,2], Deendarlianto[3] & Wiratni Budhijanto[1,2,*]

[1]Department of Chemical Engineering, Faculty of Engineering, Universitas Gadjah Mada, Jalan Grafika 2, Kampus UGM, Yogyakarta 55281, Indonesia
[2]Bioresource Engineering Group, Universitas Gadjah Mada, Jalan Grafika 2, Kampus UGM, Yogyakarta 55281, Indonesia
[3]Department of Mechanical and Industrial Engineering, Faculty of Engineering, Universitas Gadjah Mada, Jalan Grafika 2, Yogyakarta 55281, Indonesia
*E-mail: wiratni@ugm.ac.id

Highlights:

- The micro-bubble generator (MBG) is an effective aerator with higher energy efficiency compared to widely used aerators.
- The performance of an MBG depends on two operating variables, i.e. the liquid flow rate (Q_L) and the air flow rate (Q_G).
- The experiment showed that the effect of Q_L is more significant than the effect of Q_G.

Abstract. The micro-bubble generator (MBG) is a novel aeration technology utilizing the concept of fluid flow through an orifice, where air is sucked into the internal chamber of the MBG by the pressure difference created by the orifice and immediately pushed by the high-velocity flow of the fluid. This mechanism creates micro-size bubbles with a high dissolution rate. This study focused on studying the effect on the oxygen dissolution rate of the two most important operating parameters, i.e. the volumetric flow rate of the liquid (Q_L) and the volumetric flow rate of the air (Q_G). Various combinations of values for Q_L and Q_G were systematically compared by means of the oxygen mass transfer coefficient (k_La). The experiment was carried out in a transparent container of 2.8 m x 0.6 m x 0.4 m filled with tap water that was aerated using an orifice/porous-pipe type MBG. The dissolved oxygen (DO) values were measured at distances of 60 cm, 120 cm, and 180 cm from the MBG outlet. The experiment was designed with five different values for Q_L and Q_G respectively. The results showed that the value of k_La, which is proportional to the oxygen dissolution rate, increased asymptotically with increasing Q_L value, while the Q_G values did not significantly affect the k_La value.

Keywords: *aeration; dissolved oxygen; mass transfer coefficient; micro-bubble generator; orifice.*

Received January 17th, 2019, 1st Revision June 18th, 2019, 2nd Revision August 29th, 2019 , Accepted for publication March 12th, 2020.
 ISSN: 2337-5779,
DOI: 10.5614/j.eng.technol.sci.2020.52.2.5

1 Introduction

Dissolved oxygen is an important parameter in many industrial practices, such as wastewater treatment and aquaculture practices. The micro-bubble generator (MBG) is a novel aeration technology that takes advantage of the Bernoulli principle of fluid mechanics. Liquid is forced to flow through a narrowing channel created by inserting an orifice into a pipe so that the superficial velocity of the fluid increases significantly. Consequently, at the point of highest linear velocity, the pressure will drop to the lowest level into vacuum condition. Air is let in at this point by natural suction due to the pressure difference between the atmosphere and the vacuum created by the orifice. The entering air is immediately pushed by the high-velocity stream of liquid, breaking it down into micro-size bubbles. The small diameter of the bubbles leads to a higher solubility rate of the oxygen.

Several types of MBG have been published, such as the swirl-flow type introduced by Ohnari [1], the spherical body type by Sadatomi, *et al.* [2], the orifice/porous-pipe type by Sadatomi, *et al.* [3], and several other variations. Previous experience in our research group suggests that the orifice/porous-pipe MBG is the most convenient type to be applied in terms of design simplicity and easy maintenance. However, the physical design of the MBG must be accompanied by careful consideration of the process parameters to take the most advantage of the MBG in supplying oxygen. The most likely influential parameters to influence the hydrodynamics of micro-bubble formation are the characteristics of the liquid (viscosity, surface tension, and density), the liquid flow rate, and the air suction flow rate.

As published by Parmar and Majumder [4], micro-bubbles have unique characteristics, such as a slow rise velocity, a high oxygen dissolution rate, and a large gas-liquid interfacial area. These characteristics make MBG a very attractive aeration technology. Budhijanto, *et al.* [5] has published a preliminary study on MBG (orifice/porous-pipe type) application in tilapia fish (*Oreochromis niloticus*) aquaculture. Deendarlianto, *et al.* [6] applied MBG as an aerator in wastewater treatment. Iriawan, *et al.* [7] has confirmed that MBG reaches the same dissolved oxygen (DO) level with lower energy consumption compared to conventional aerators. Besides, the coverage area that can be managed to maintain the same level of DO is also wider with an MBG as aerator.

All previous studies presented evidence of the potential use of an MBG as an effective aerator with higher energy efficiency compared to widely used aerators. Nevertheless, deeper study is needed to establish stronger theoretical support in order to make better engineering judgments in applying MBGs for various purposes. The aforementioned studies applied MBGs with trial-and-error in terms

of configuration and operating parameters, such as the combination of liquid flow rate and gas flow rate. Meanwhile, other studies, such as Sadatomi, *et al.* [3], mostly describe MBG performance in terms of random operating parameters in order to prove that micro-bubbles were generated.

The current study was focused on finding the best combination of selected operating parameters, i.e. the liquid flow rate circulated into the MBG (Q_L) and the gas flow rate into the MBG (Q_G), with evaluating the sensitivity of MBG performance. Studies concerning a method to systematically optimize process parameters in MBG application are still very limited, which is one of the challenges in MBG development. This paper presents a mass-transfer approach to defining the performance of the MBG and hence provide a more practical tool for optimizing the MBG configuration. Specifically, this study aimed to evaluate the effect of the liquid flow rate (Q_L) and the air flow rate (Q_G) on the bubble size distribution and the rate of oxygen dissolution at several distances from the MBG outlet.

2 Methods

This research used an orifice/porous-pipe type MBG (Figure 1) designed and fabricated by Fluid Mechanics Laboratory Group, Department of Mechanical and Industrial Engineering, Faculty of Engineering, Universitas Gadjah Mada. The modification of this MBG compared to the original design of Sadatomi, *et al.* [3] uses a ceramic porous pipe. The porous pipe through which the air is sucked into the orifice chamber was made of a custom-made plastic scaffold and nylon fibers rolled around the scaffold. This customization of the porous pipe increases its durability and reduces the manufacture cost.

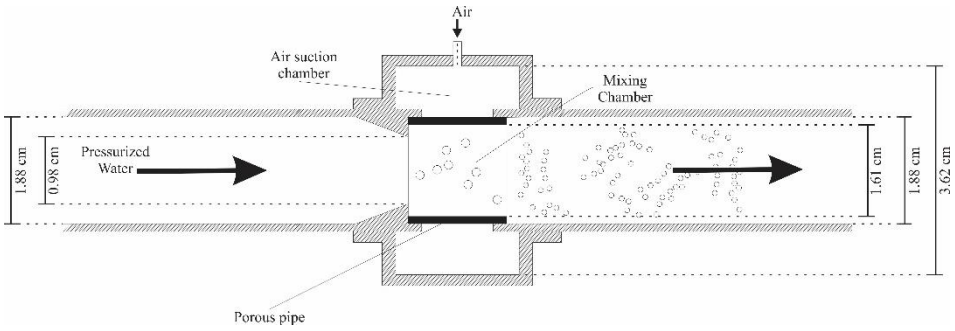

Figure 1 Schematic diagram of the orifice/porous-pipe MBG.

The MBG was installed in a transparent-walled container with dimensions of 280 cm x 60 cm x 40 cm, with the experimental set-up shown in Figure 2. The

MBG was installed at a depth of 20 cm under the water surface, located on one end of the container.

The container was filled with clear tap water. A DO meter was secured in place to measure the DO level in the container. The initial DO level without aeration was ±3 mg/L. The variations in Q_L were set by adjusting the pump rotation rate, while Q_G was set manually by adjustment of the gas flow meter valve.

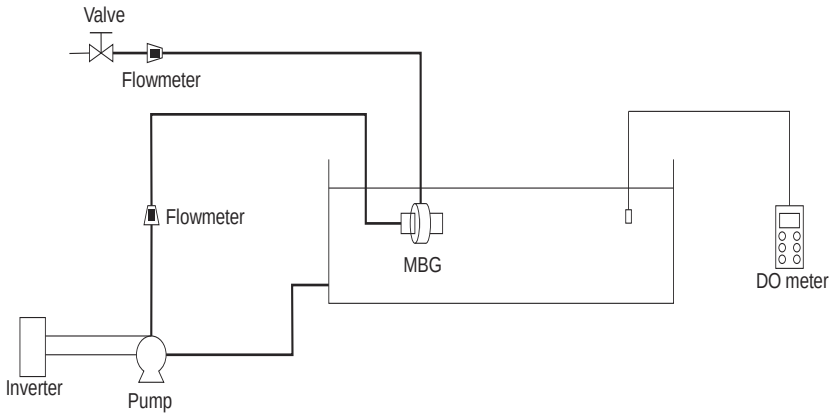

Figure 2 Schematic diagram of the experimental set-up.

Aeration was done with various combinations of Q_L and Q_G according to the experimental design presented in Table 1. DO measurements were taken using a data logger at 3-second intervals for 1.5 minutes, at distances of 60 cm, 120 cm, and 180 cm from the MBG outlet. DO measurements were taken three times for each combination of Q_L and Q_G.

Table 1 Experimental design for Q_L and Q_G combinations in this study.

Q_G (LPM)	**Q_L (LPM)**				
	(1)	(2)	(3)	(4)	(5)
0.2	30	40	50	60	70
0.4	30	40	50	60	70
0.6	30	40	50	60	70
0.8	30	40	50	60	70
1.0	30	40	50	60	70

The bubble size distribution was measured by means of image processing of a visual record of the bubbles. The method used is called the shadow image technique, referring to the previous study by Majid, *et al.* [8] for analyzing horizontal co-current gas-liquid plug two-phase flow. Basically, this technique puts the bubbles between a camera and a screen with a light source on the opposite

side (Figure 3). Bubbles create dark spots on the screen, which are then captured by the camera (Phantom high speed with a maximum frame rate of 10,000 frames per second/fps). Camera adjustment included recording speed at 3000 fps, aperture at 2.8, and focal length of the lens at 85 cm. With these conditions, an object at 40 cm distance from the lens has a focal depth of 3 cm. A calibration plate was inserted into the water container prior to bubble recording to obtain the best focus. The background image was obtained by recording an image of the container without the presence of bubbles. Digital image processing was conducted using Matlab 2016a equipped with Image Processing Toolbox. The results are presented as the probability density function (PDF).

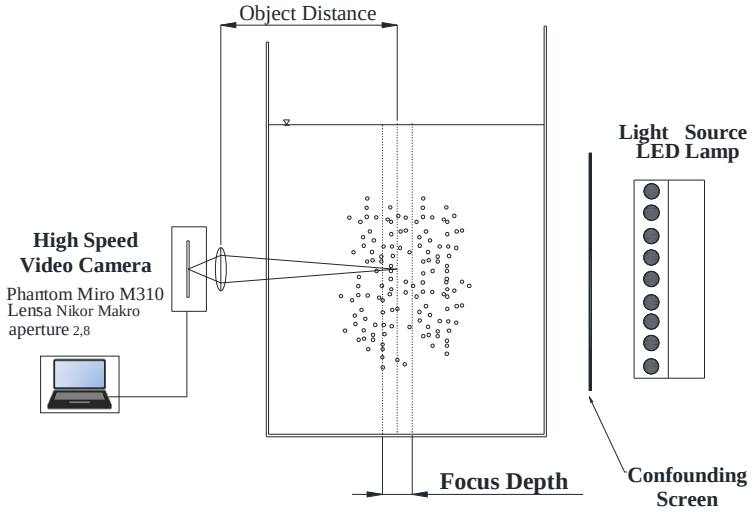

Figure 3 Schematic diagram of image recording technique.

The oxygen dissolution rate was quantified using a simplified model of the oxygen mass transfer rate presented in Eq. (1). The parameters compared between the various combinations of Q_L and Q_G were the values of k_La obtained as the negative slope of the linear correlation presented in Eq. (2).

$$\frac{dC_{DO}}{dt} = k_L a\left(C^*_{DO} - C_{DO}\right) \tag{1}$$

$$ln\frac{\left(C^*_{DO} - C_t\right)}{\left(C^*_{DO} - C_0\right)} = -k_L a t \tag{2}$$

$$C^*_{DO} = 0.0032T^2 - 0.3316T + 14.657 \tag{3}$$

where k_La is the volumetric mass transfer coefficient (1/second), C^*_{DO} is the saturated dissolved oxygen concentration in water (mg/L) empirically correlated with temperature in Eq. (3); C_t is the concentration of dissolved oxygen at a particular time t (measured by DO meter in mg/L); and C_0 is the initial concentration of dissolved oxygen in the water (mg/L).

3 Results and Discussion

3.1 Bubble Size Distribution

Figure 4 exhibits the average bubble diameter for the various combinations of Q_L and Q_G tested in this study. Increasing Q_L reduced the average bubble size. This observation is in good accordance with the work of Khirani, *et al.* [9]. The turbulence induced by a higher Q_L improved the bubble breakdown mechanism in the orifice chamber, resulting in smaller bubbles. On the other hand, increasing Q_G had the opposite effect, i.e. increasing the bubble size. This tendency was also observed in the previous study by Majid, *et al.* [10].

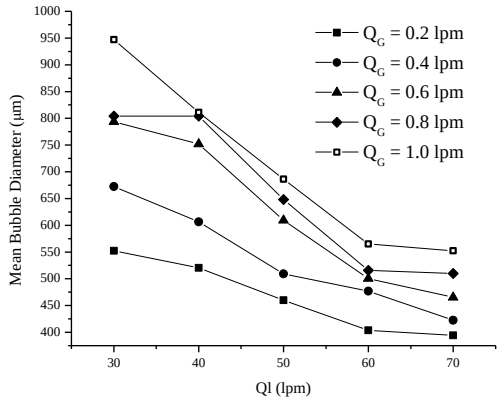

Figure 4 Average bubble diameters at various combinations of Q_L and Q_G.

Deeper insight into the bubble size distribution was obtained by observing the bubble size distribution plots in Figure 5. In general, increasing Q_G resulted in a wider distribution curve. This reflects more heterogeneous bubble sizes when Q_G was increased. According to Lau, *et al.* [11], a higher Q_G causes increasing numbers of bubbles with larger sizes, which move more rapidly towards the water surface compared to slow-moving micro-bubbles. The fast rising bubbles tend to collide with each other and hence create even larger sized bubbles.

On the other hand, increasing Q_L led to a narrower distribution, which implies a more homogeneous bubble size, in the range of 100 to 300 microns. Changjun, *et al*. [12] have reported that the dominant forces controlling micro-bubble formation are the surface tension and the inertial force of the liquid.

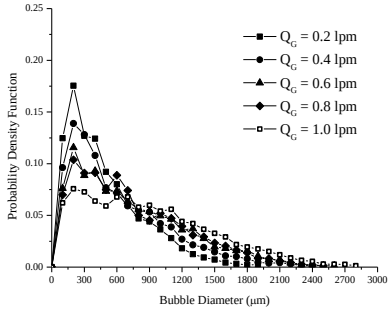

(a) Q_L = 30 lpm

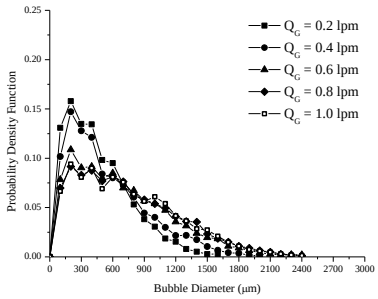

(b) Q_L = 40 lpm

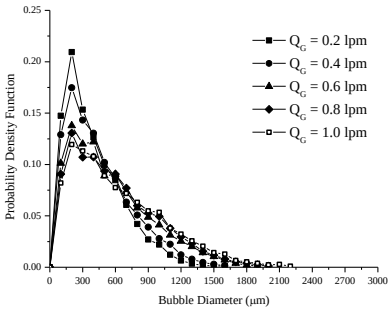

(c) Q_L = 50 lpm

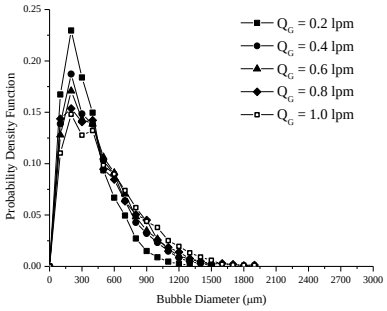

(d) Q_L = 60 lpm

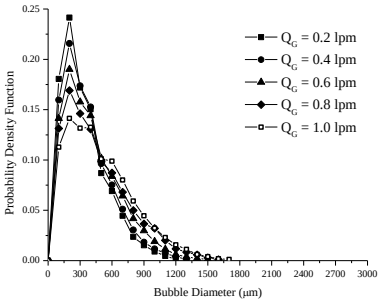

(e) Q_L = 70 lpm

Figure 5 Bubble size distribution at various combinations of Q_L and Q_G.

The surface tension is responsible for bubble size stability, while the inertial force governs the behavior of the bubble in the liquid stream. This theory is the basic reference to explain the effects of Q_L and Q_G on the micro-bubble size distribution. When Q_G is increased relative to Q_L, the volume of the bubbles will grow to compensate for the additional mass of gas in the same pressure balance created by the surface tension. On the other hand, when Q_L is increased relative to Q_G, the inertial forces around the bubbles will increase to break the surface tension force so that the bubbles tend to be smaller and disappear more quickly, either by dissolution or by being taken out of the system by the liquid flow.

According to all plots in Figure 5, the highest probability of occurrence was observed in the range of 100-300 µm, accounting for 15-30% of the total bubbles captured by the camera. However, we should take into account that the speed of the camera may have been insufficient to capture all the bubbles in the system, specifically those that existed less than 1/3000 seconds. This portion of fast disappearing bubbles may be high in MBG aeration systems that produce very small bubbles with a high dissolution rate.

With such uncertainty in bubble size distribution data due to the limitations of the camera, it is necessary to conduct another measurement to define the performance of the MBG. As dissolved oxygen is the main target of this aeration process, the logical parameter to determine the success of the aeration process is the oxygen mass transfer coefficient (k_La) defined by Eq. (2). The higher the k_La values, the more preferable the aeration condition. Hence, the combination of Q_L and Q_G should be chosen so that the highest possible value of k_La is obtained. The next section presents a discussion of the effects of various combination of Q_L and Q_G on the values of k_La.

3.2 Volumetric Mass Transfer Coefficient (k_La)

The values of k_La were obtained based on data fitting on Eq. (2). Figure 6 presents the values of k_La for various combinations of Q_L and Q_G. The measurement of DO was taken at a distance of 60 cm from the MBG outlet. The most interesting fact was that the values of k_La increased with increasing Q_L, but did not significantly change with increasing Q_G. Compared to Figure 5, although the bubble size distribution seems similar for all combinations of Q_L and Q_G, it turns out that the oxygen dissolution behaviors were quite different with those combinations.

According to a widely accepted theory on transport phenomena stated by Bird, *et al.* [13], a higher Q_L value leads to a higher k_La due to increased turbulence, which reduces the interface resistance for any mass transfer across an interface. This is the reason why increasing Q_L from 30 to 60 lpm significantly increased the k_La

values. Increasing Q_L further to 70 lpm did not significantly increase the k_La value anymore because the concentration of dissolved oxygen had reached its saturation point. The effect of Q_L was more dominant than that of Q_G with respect to creating turbulence in the MBG, which is required to enhance k_La. Therefore, Q_G is less influential on the values of k_La compared to the effect of Q_L on k_La.

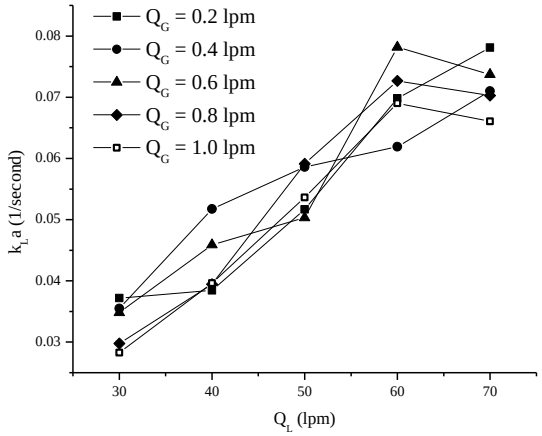

Figure 6 Values of k_La at various combinations of Q_L and Q_G.

Figure 6 confirms that Q_L has a more profound effect on k_La. Therefore, the evaluation of the effect on distance was only conducted with variation of Q_L. Figure 7 shows that at 180 cm distance from the MBG outlet, the k_La value decreased significantly. At this position, the effect of Q_L was not as large as at other positions. A possible explanation for this behavior is that beyond 120 cm from the MBG outlet, the oxygen transfer is not effective anymore. This preliminary study merely highlighted that it is important to determine the farthest distance reached by the micro-bubbles, because beyond this critical distance, the aeration is not effective at all. A more detailed calculation of such critical distance is beyond the scope of this study; it needs to be modeled to determine the optimum configuration/position of the MBG installation.

It is worth mentioning that an optimum Q_L value could be determined based on this study. A Q_L value of 60 lpm was considered optimum because increasing it to 70 lpm did not change the k_La value and hence with respect to energy consumption. Thus, there was no use in supplying more energy to make Q_L higher than 60 lpm.

The aforementioned analysis on the effects of Q_L, Q_G and distance from MBG outlet on the k_La values was crosschecked using two-way analysis of variance (ANOVA). The ANOVA calculation is presented in Table 2. Significant effects

are represented by a p-value smaller than 0.05. Based on Table 2, Q_L, distance, and the interaction of both had significant effects.

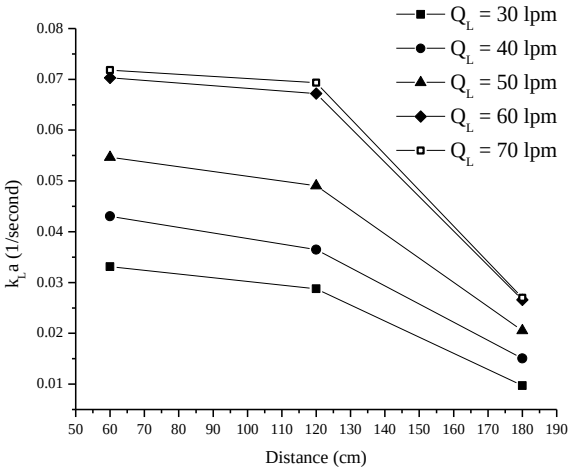

Figure 7 Values of k_La at various Q_L values and distances from the MBG outlet.

Table 2 Analysis of variance for the effects of Q_L, Q_G, and distance on k_La values.

Source	Adjusted sum of squares	Adjusted mean squares	F-value	P-value
Q_L	0.034493	0.034493	395.50	**0.000**
Q_G	0.000012	0.000012	0.14	0.710
X	0.045498	0.045498	521.67	**0.000**
Q_L*Q_G	0.000057	0.000057	0.65	0.421
Q_L*X	0.002576	0.002576	29.54	**0.000**
Q_G*X	0.000138	0.000138	1.59	0.209

4 Conclusion

Affordable formation of bubble size in the micron range is the purpose of micro-bubble generator (MBG) technology. This study presented a systematic method to evaluate the performance of an MBG in terms of bubble size distribution and oxygen mass transfer coefficient.

In the micrometer range, bubble size measurement is limited by the capability of the camera to capture bubble formation, which may take a very short time, making it impossible to be captured by camera. However, the bubble size distribution measured in this study yielded the general finding that a higher Q_L

value led to a smaller average bubble size, while a higher Q_G value induced a larger average bubble size. Besides, increasing Q_L relative to Q_G tended to homogenize the bubble size, hence narrowing the bubble size distribution curve. On the other hand, increasing Q_G relative to Q_L caused a wider size distribution curve, which indicates a more heterogeneous bubble size.

The value of mass transfer coefficient (k_La) is the most appropriate option to define MBG performance because it is determined based on accurate data of dissolved oxygen over a certain period of time. It was shown that k_La values were significantly affected by Q_L and distance from the MBG outlet. A higher value of k_La indicates better MBG performance in supplying dissolved oxygen and could be achieved at higher Q_L. It should be noted that an optimum Q_L was determined, above which the value of k_La could not be increased anymore as saturation was already reached. With respect to distance from the MBG outlet, a critical distance was observed. At points farther than this critical distance, the value of k_La dropped significantly.

Acknowledgements

This research was funded by a competitive research grant from *Penelitian Unggulan Perguruan Tinggi* (PUPT) 1934/UN1/DITLIT/DIT-LIT/LT/2018 with Dr. Deendarlianto as the principal investigator.

References

[1] Ohnari, H., *Swirling Fine-Bubble Generator*, US 6382601 B1, US Patent, 2002.

[2] Sadatomi, M., Kawahara, A., Kano, K. & Ohtomo, A., *Performance of New Micro-bubble Generator with a Spherical Body in a Flowing Water Tube*, Experimental Thermal and Fluid Science, **29**, pp. 615-623, 2004.

[3] Sadatomi, M., Kawahara, A., Matsuura, H. & Shikatani, S., *Micro-bubble Generation Rate and Bubble Dissolution Rate into Water by a Simple Multi-fluid Mixer with Orifice and Porous Tube*, Experimental Thermal and Fluid Science, **41**, pp. 23-30, 2012.

[4] Parmar, R. & Majumder, S.K., *Micro-bubble Generation and Microbubble-Aided Transport Intensification – A State-of-the-Art Report*, Chemical Engineering and Process: Process Intensification, **64**, pp. 79-97, 2013.

[5] Budhijanto, W., Darlianto, D., Pradana, Y.S. & Hartono, M., *Application of Micro Bubble Generator as Low Cost and Highly Efficient Aerator for Sustainable Fresh Water Fish Farming*, AIP Conference Proceedings, **1840**(1), 110008, 2017. DOI: 10.1063/1.4982338.

[6] Deendarlianto, Wiratni, Tontowi, A.E., Indarto, & Iriawan, A.G.W., *The Implementation of a Developed Microbubble Generator on the Aerobic Wastewater Treatment*, International Journal of Technology, **6**(6), pp. 924-930, 2015.

[7] Iriawan, A.G.W., Tohani, A., Deendarlianto, Wiratni, Tontowi, A.E. & Widyaparaga, A., *Experimental Study on Optimization the Suction Volume Air and the Axial Position of the Spherical Body on the Microbubble Generator in A Flowing Water Tube*, Proceedings of the 8th International Conference on Multiphase Flow, Jeju Island, January 2013.

[8] Majid, A.I., Dinaryanto, O., Deendarlianto, & Indarto, *Quantitative Visualization of the Wave Characteristics for Horizontal Co-current Gas-liquid Plug Two-phase Flow by Using an Image Processing Technique*, Proceeding of Seminar Nasional Thermofluid VI, Yogyakarta, April 2014.

[9] Khirani, S., Kunwapanitchakul, P., Augir, F., Guigui, C., Guiraud, P. & Hebrard, G., *Microbubble Generation through Porous Membrane Under Aqueous or Organic Liquid Shear Flow*, Industrial & Engineering Chemistry Research, **51**(4), pp. 1997-2009, 2012.

[10] Majid, A.I., Nugroho, F.M., Juwana, W.E., Budhijanto, W., Deendarlianto, & Indarto, *On the Performance of Venturi-Porous Pipe Microbubble Generator with Inlet Angle of 20 and Outlet Angle of 12*, AIP Conference Proceedings of the International Workshop on Advanced Materials (IWAM-2017), India, August 2017.

[11] Lau, Y.M., Deen, N.G. & Kuipers, J.A.M., *Development of An Image Measurement Technique for Size Distribution in Dense Bubbly Flows*, Chemical Engineering Science, **94**, pp. 20-29, 2013.

[12] Changjun, L., Bin, L., Shengwei, T. & Haiguang, Z., *A Theoritical Model for the Size Prediction of Single Bubble Formed under Liquid Cross Flow*, Chinese Journal of Chemical Engineering, pp. 770-776, 2010.